

RESEARCH PAPER

## Polyvinyl Pyrrolidone/Nickel Oxide (PVP/NiO) Nanocomposite: Synthesis, Characterization, and Removal Study of Eosin Y Using Adsorption Process

Aliakbar Dehno Khalaji\*, Emad Jafari, Moslem Emami, Negin Mohammadi

Department of Chemistry, Faculty of Science, Golestan University, Gorgan, Iran

### ARTICLE INFO

#### Article History:

Received 31 May 2023

Accepted 03 Sep 2023

Published 01 Oct 2023

#### Keywords:

PVP/NiO nanocomposite,

Removal,

Eosin Y,

Adsorption capacity.

### ABSTRACT

In this study, the PVP/NiO nanocomposite was synthesized using the solution cast technique and characterized by Fourier transform infra-red (FT-IR), X-ray powder diffraction (XRD), thermogravimetric analysis (TGA), differential thermal analysis (DTA), energy-dispersive X-ray spectroscopy (EDS), and scanning electron microscope (SEM). The results confirmed the successful preparation of PVP/NiO. The as-prepared PVP/NiO was used as a new adsorbent for the removal of eosin Y (EY) dye from aqueous solution at room temperature. The effect of different important parameters such as solution pH, adsorbent dose, and contact time on the adsorption efficiency of EY was investigated. The maximum adsorption capacity was found to be 101.58 mg/g at the initial pH solution of 3, 0.025 g adsorbent dose, and 90 min of contact time. The kinetic study indicated that the remove of EY was followed by a pseudo second-order (PSO) model. Then, the as-prepared PVP/NiO possessed well adsorption potential for the removal of other organic dyes from aqueous solution.

### How to cite this article

Dehno Khalaji A., Jafari E., Emami M., Mohammadi N., Polyvinyl Pyrrolidone/Nickel Oxide (PVP/NiO) Nanocomposite: Synthesis, Characterization, and Removal Study of Eosin Y Using Adsorption Process. *Nanochem. Res.*, 2023; 8(4): 258-266. DOI: 10.22036/NCR.2023.04.04

### INTRODUCTION

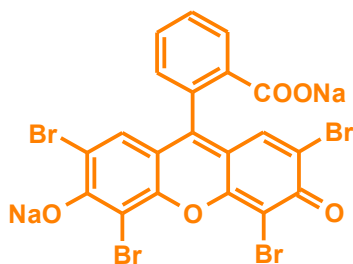
Organic dyes containing azo group and aromatic rings are very toxic, stable, non-biodegradable, and carcinogenic. They were used as colorants in various industries such as leather, food, paper, and textile [1]. The discharge of industrial wastewater into the nearby water source causes the pollution of aquatic systems [2], which may lead to cancers, tumors, allergies, and mutations in humans [3]. Thus, the industrial wastewater should be treated before its discharge into the environment using different techniques [4-8]. Among them, the adsorption process is one of the most important techniques for the removal of organic dyes using various compounds as adsorbents due to being simple, low cost, highly efficient, and without

second pollution [9-12].

Eosin Y (EY) as anionic dye (Scheme 1) is a pink colored which exhibits yellow green fluorescence and is widely used in the Gram straining of the bacterial strain [13]. In addition, eosin Y is used in dyeing, printing, and paints factory [14]. However, it causes damages to liver, lungs, eyes, skin, and kidneys [13]. Until now, various techniques have been available for the removal of eosin Y dye from aqueous solutions [15-17]. However, removing organic dyes using adsorption process has been widely used due to its low cost, simplicity and high efficiency [18-20]. Various solid materials are used as adsorbent for the removal of organic dyes such as transition metal oxide nanoparticles [21,22] as well as their polymeric nanocomposites [23-25]. In recent years, the adsorption process was performed

\* Corresponding Author Email: [alidkhalaji@yahoo.com](mailto:alidkhalaji@yahoo.com)





Scheme 1. Chemical structure of eosin Y dye

to remove different organic dyes by modifying various polymers such as PVA [26], modified chitosan [27-29], and PVP [30-32].

Poly(vinyl pyrrolidone) (PVP) is a water-soluble synthetic homopolymer; it is also neutral, biodegradable, low cost, non-toxic, hydrophilic, and biocompatible, which has numerous potential applications [33-39] such as the delivery of drugs [40], removal of organic dyes [30-32], and pharmaceutical formulations [41]. Moreover, polyvinylpyrrolidone (PVP) can be extensively used in order to prevent particle aggregation and control the average particle size and shape of nanoparticles [42]. The incorporation of transition metal oxide into a PVP matrix can improve the chemical and physical properties [33-39, 43].

In the present paper, we synthesized PVP/NiO nanocomposite via the co-precipitation technique and characterized. In addition, the adsorption study was examined for the removal of eosin Y (EY) dye from aqueous solution.

## EXPERIMENTAL

All reagents, such as polyvinyl pyrrolidone (PVP) and eosin Y, were purchased from Merck Co. NiO nanoparticles were prepared according to the previous literature [27]. FT-IR spectrum of PVP/NiO was recorded by spectrophotometer instrument (Perkin-Elmer) (KBr disks, 4000–400  $\text{cm}^{-1}$ ). X-ray diffractometer ( $2\theta = 10\text{-}80^\circ$ , Bruker AXS-D8) was applied to determine XRD pattern. DSC analysis was recorded by a DSC analyzer (Model 60A, Shimadzu, Japan). FE-SEM images were recorded on the TESCAN Vega Model scanning electron microscope. UV-Vis spectra were carried out with a UV-Visible spectrophotometer (Perkin-Elmer).

1 g of PVP was suspended in 10 mL of ethanol and stirred for 10 min. Then, 0.25 g of NiO nanoparticles was added and magnetically stirred for 6 h. After the evaporation of the solvent, the gray

precipitates were washed twice with distilled water, then dried at room temperature and characterized.

The EY dye adsorption capacity was evaluated by placing 0.012 and 0.025 g of PVP/NiO in 70 mL of a 20 mg/L EY dye aqueous solution at room temperature. The pH of the EY solutions was adjusted using 0.1 M NaOH or 0.1 M HCl until the desired pH (2–11) was obtained. At predetermined time intervals (0–90 min), 3 mL of the solutions were sampled to evaluate the EY content residual in the solution by UV-vis spectroscopy. The dye content in the supernatant solution was obtained by measuring the sample's absorptivity. The analyses of EY dye adsorption capacities were conducted using the following equation:

$$R (\%) = \frac{C_i - C_t}{C_i} \times 100 \quad (1)$$

$$q_t (\text{mg/g}) = \frac{(C_i - C_t) \times V}{M} \quad (2)$$

where, R is the removal percentage and  $q_t$  is the amount of EY dye adsorbed at different contact time;  $C_i$  represents the initial concentration of EY dye (mg/L);  $C_t$  denotes EY concentration at different contact time (mg/L); V is the volume of the EY dye solution (L), and M is the mass of PVP/NiO (g).

## RESULTS AND DISCUSSION

### FT-IR

The FT-IR spectra of PVP and PVP/NiO nanocomposite are presented in Fig. 1. PVP and PVP/NiO demonstrate a broad peak at about 3450  $\text{cm}^{-1}$  assigned to O-H band and also adsorbed water molecules [44-47]. Additionally, a peak at 1675  $\text{cm}^{-1}$  is assigned to the C=O absorption bands [33-39]. The peaks at about 2950  $\text{cm}^{-1}$  are ascribed to the symmetric  $\text{CH}_2$  stretching [33-39], while the band at about 1440  $\text{cm}^{-1}$  is attributed to the  $\text{CH}_2$  bending [33-39]. A sharp peak at 441  $\text{cm}^{-1}$  in PVP/NiO is assigned to the Ni-O stretching mode [44-47].

### XRD

The XRD patterns of PVP and PVP/NiO nanocomposite are shown in Fig. 2. PVP shows two broad peaks at 11 and 20° and these peaks are observed in PVP/NiO at  $2\theta$  of 11.5 and 21°. The intensity of the peaks in PVP/NiO is lower than that of similar peaks in pure PVP and NiO nanoparticles, indicating a decrease in the crystallinity of the synthesized PVP/NiO compound [44-47]. In addition, in the XRD pattern of NiO/PVP, there

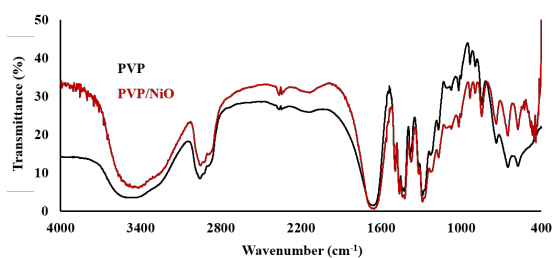


Fig. 1. FT-IR spectra of NiO, PVP and PVP/NiO nanocomposite

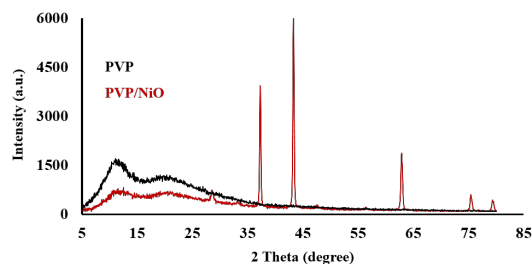


Fig. 2. XRD patterns of PVP and PVP/NiO nanocomposite

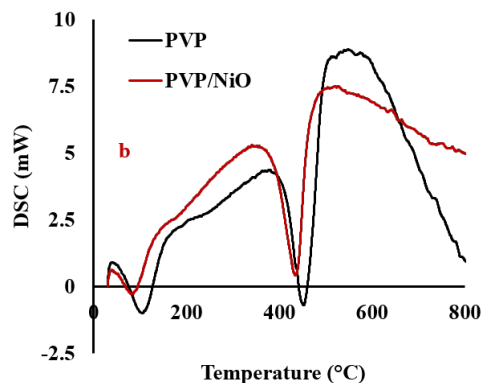
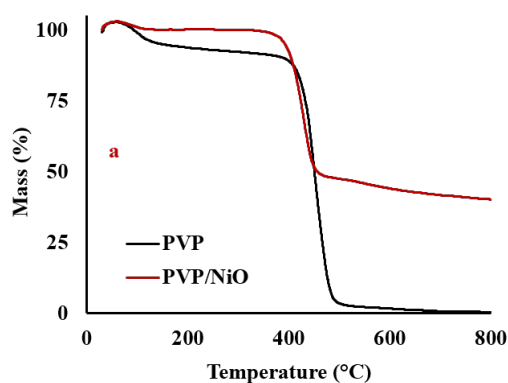


Fig. 3. a) TGA curves and b) DSC thermograms of PVP and PVP/NiO nanocomposite

are five sharp and narrow peaks at  $2\theta$  of 37.3, 43.4, 63.1, 75.6 and 79.5°, corresponding to (111), (200), (220), (311) and (222) crystal planes of cubic NiO (JCPDS card no. 47-1049) [44-47], confirming the successful preparation of PVP/NiO nanocomposite.

#### TGA-DSC

TGA and DSC curves of PVP and PVP/NiO nanocomposite are presented in Fig. 3. PVP and PVP/NiO show a mass loss of  $\approx 7\%$  and  $\approx 3\%$ , respectively, in the first stage at about 100 °C, assigned to the removal of moisture and water molecules adsorbed. Their mass losses at temperatures up to  $\approx 365$  °C for PVP/NiO and 410 °C for PVP are almost negligible. After that and up to 450 °C, PVP and PVP/NiO nanocomposite show a mass loss of 91% and 52%, respectively. Finally, at 800 °C, the remaining mass of PVP and PVP/NiO is  $\approx 0\%$  and  $\approx 45\%$ , respectively. The mass loss of PVP and PVP/NiO can be explained in more detail by DSC thermogram (Fig. 3b). A mass loss process observed at 105 and 80 °C for PVP and PVP/NiO, which indicates the evaporation of moisture or water molecules. A sharp peak related to the main decomposition stage of PVP and PVP/NiO was seen at 453 and 435 °C, respectively [39,43].

#### SEM-EDS

SEM images of PVO and PVP/NiO nanocomposite are presented in Fig. 4. PVP has an almost smooth surface with varying particle sizes and also particles are stacked on top of each other. By adding NiO nanoparticles to PVP, many number of pores have been created between the PVP particles, which enhances the interaction between the EY molecules with PVP/NiO and can provide a large number of active adsorption sites. The NiO nanoparticles are spherical in shape, with a particle size ranging from 40-70 nm.

EDS spectra of PVP and PVP/NiO nanocomposite are shown in Fig. 5. It can be seen that the contents of C and H of PVP simultaneously decreased, while the O and Ni contents increased, indicating the successful deposition of NiO onto the PVP polymer and preparation of PVP/NiO nanocomposite.

#### Adsorption study of eosin Y (EY)

The adsorption of eosin Y (EY) was investigated by UV-Vis spectrophotometer in order to measure the absorbance intensity in 520 nm using PVP/NiO. Fig. 6 illustrates the maximum absorbance of EY solution after different contact time at

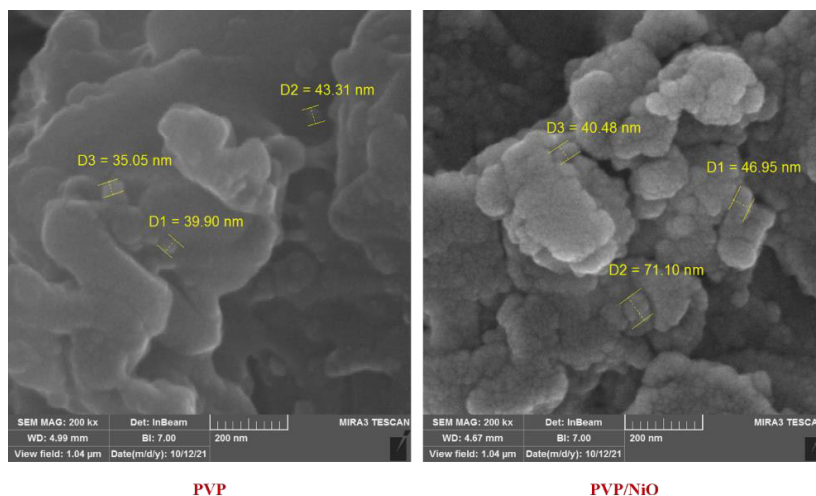


Fig. 4. SEM images of PVP and PVP/NiO nanocomposite

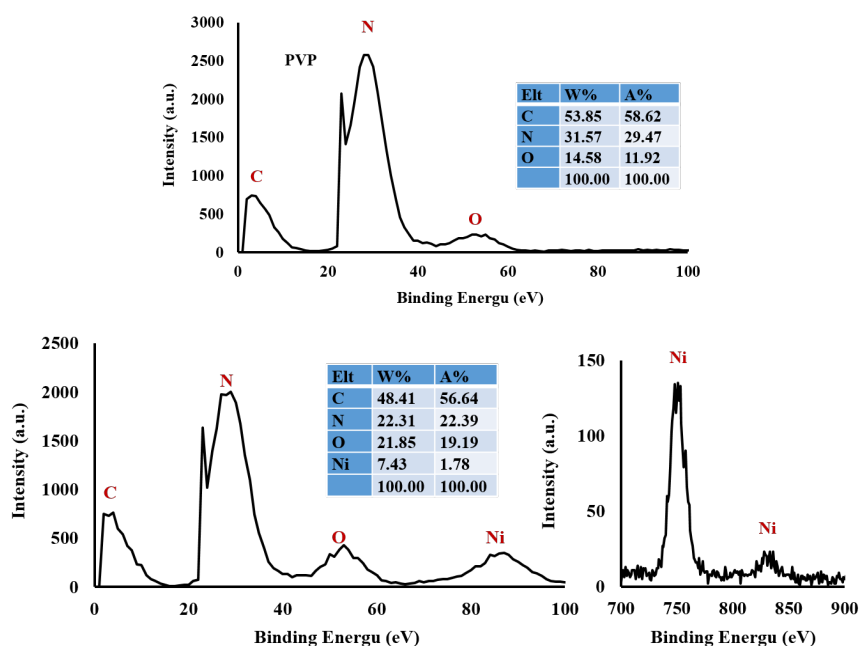


Fig. 5. EDS spectra of a) PVP and b) PVP/NiO nanocomposite

the presence of various doses of PVP/NiO, and shows the decrease of absorbance intensity by increasing contact time, confirming that the removal of EY from aqueous solution by PVP/NiO nanocomposite.

In the removal of different organic dyes from the aqueous solution, the solution pH plays an important role in the adsorption process due to controlling the surface charge of adsorbent [20]. In this paper, the effect of pH on the removal efficiency of EY using PVP/NiO was studied in

the pH range of 3-5 as shown in Fig. 7. It is seen that the removal efficiency of EY decreases with increasing pH [1,2,48], and about 99.98% removal is obtained at pH 3 in the presence of 0.025 f of PVP/NiO.

Due to the protonation of the active sites on the surface of PVP/NiO at low pH, which enhances the electrostatic attraction between the PVP/NiO surface and anionic EY molecules, the removal percentage was increased [1, 2, 48]. By increasing the pH solution, the active groups of PVP/NiO

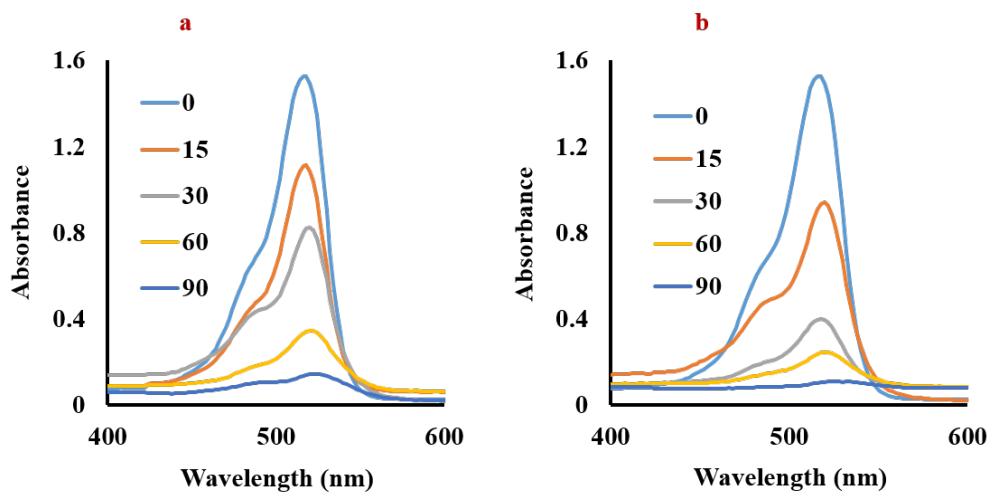


Fig. 6. The effect of time on changes of the maximum absorbance of EY solution (pH = 3, 70 mL, 20 ppm) a) 0.0125 g and b) 0.0250 g of PVP/NiO

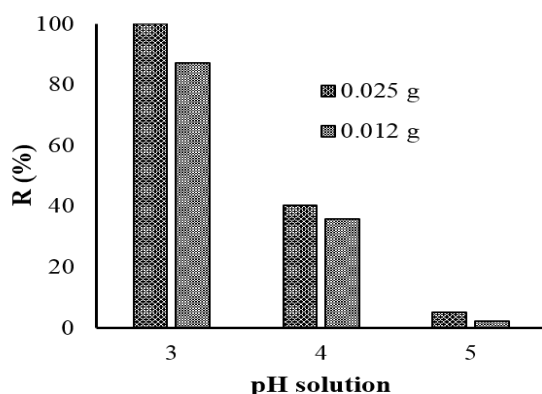


Fig. 7. The effect of pH and sorbent dose of removal percentage of EY

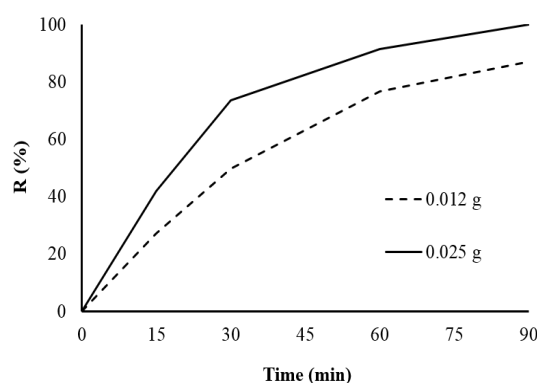


Fig. 8. The effect of contact time and sorbent dose on a) removal percentage and b) adsorption capacity of EY solution (pH = 3, 70 mL, 20 ppm)

underwent deprotonation due to the decrease of  $H^+$  ions. At the pH solution of 5, the removal percentage of EY molecule dye was found to be very low (<10%). Then, the pH solution of 3 was selected for the investigation of contact time and adsorbent dose.

The effect of PVP/NiO dose (0.012 and 0.025 g) and contact time (0 – 90 min) on the removal of EY is illustrated in Fig. 8. It can be seen that the removal percentage of EY was increased with increasing PVP/NiO due to the increase of the active sites on the surface of the sorbent as well increased contact time [1,2,48]. At optimal condition, the maximum removal percentage of EY dye reached 99.98% (Fig. 8). The maximum adsorption capacity was found to be 101.58 mg/g using 0.012 g of PVP/NiO (Fig. 8).

#### Kinetic studies

The adsorption kinetic of the removal of EY dye was studied by the first and second order models using the following equations (Figs. 9 and 10) [24,49].

$$\log(q_e - q_t) = \log q_e - (k_1/2.303)t \quad (3)$$

$$(t/q_t) = (1/k_2 q_e^2) + t/q_e \quad (4)$$

Where,  $k_1$  and  $k_2$  are the rate constants for first and second order kinetic models;  $q_e$  and  $q_t$  are EY concentration at equilibrium and particular time, respectively. As seen in Fig. 8, the kinetic linear curves showed that the adsorption of EY dye follow a pseudo second-order model [1,50].

#### Adsorption mechanism

Previous studies on the removal of different

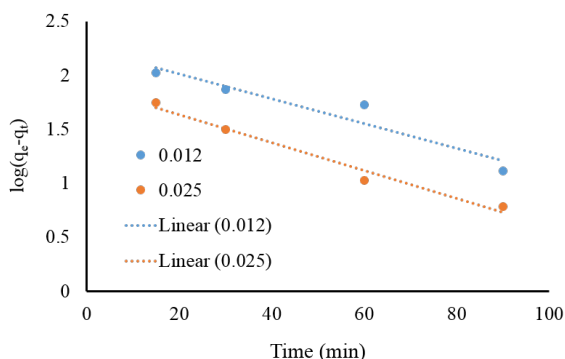


Fig. 9. The plot of pseudo first order model fit for EY adsorption using PVO/NiO

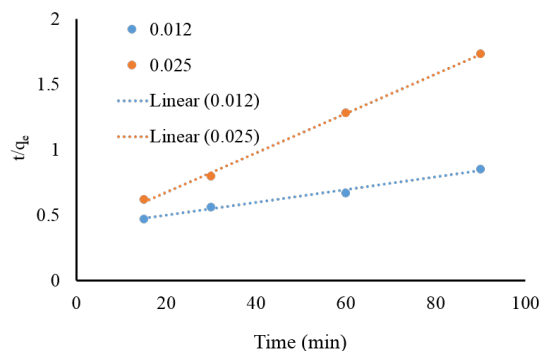
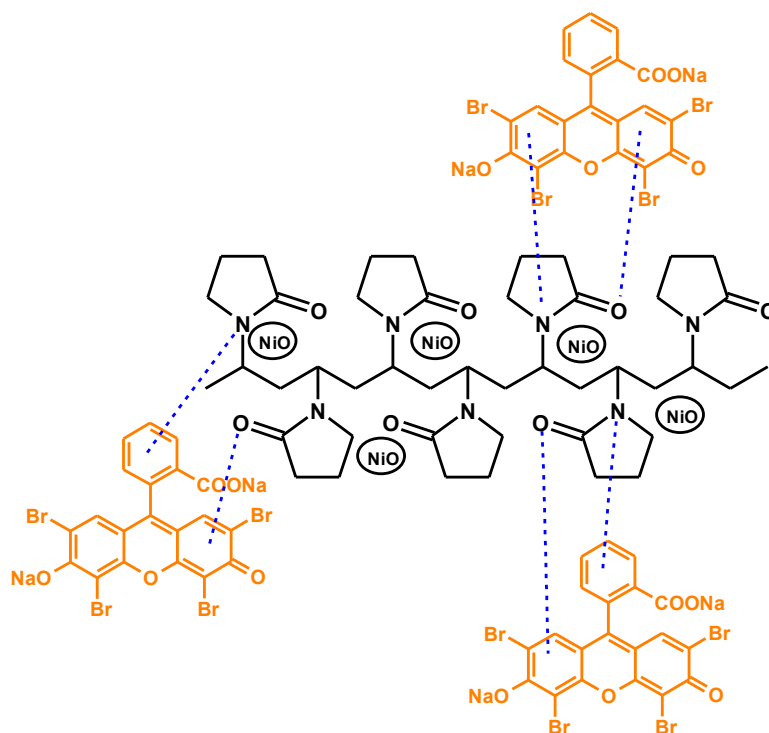


Fig. 10. The plot of second first order model fit for EY adsorption using PVO/NiO



Scheme 2. The proposed adsorption mechanism of EY on PVP/NiO nanocomposite

colors with the help of polymer composites have demonstrated that color removal is done by various interactions such as H-bonding,  $\pi$ - $\pi$  interaction, n- $\pi$  interaction, and electrostatic attraction [27-29]. According to the adsorption results of EY removal and functional groups on the surface of PVP/NiO composite, the main cause of EY dye removal is n- $\pi$  interaction, which is shown in Scheme 2. This interaction occurs between the lone-pairs of O and N electron-donation on the surface of PVP/NiO and the aromatic rings of the EY molecules.

## CONCLUSIONS

In this study, new PVP/NiO nanocomposite was synthesized, characterized and used as a new sorbent for the removal of eosin Y from aqueous solution. The results demonstrated that the maximum adsorption capacity was found to be 101.58 mg/g at pH solution of 3, using 0.0125 g of sorbent after 90 min contact time. These results reveal that the PVP/NiO could efficiently remove EY dyes. The kinetic studies showed that the adsorption of EY dyes follow a pseudo second-



order model, which involves  $n-\pi$  interaction. Thus, PVP/NiO nanocomposite could be studied as a new potential sustainable candidate for the removal of other harmful organic dyes.

#### ACKNOWLEDGMENTS

The authors are grateful to Golestan University for supporting this research.

#### CONFLICT OF INTEREST

The authors declare no conflicts of interest.

#### REFERENCES

- Thulasi singh A, P S, K S. Synthesis of nano-sized chitosan blended polyvinyl alcohol for the removal of Eosin Yellow dye from aqueous solution. *Journal of Water Process Engineering*. 2016;13:127-36. <https://doi.org/10.1016/j.jwpe.2016.08.003>
- Haldorai Y, Shim J-J. An efficient removal of methyl orange dye from aqueous solution by adsorption onto chitosan/MgO composite: A novel reusable adsorbent. *Applied Surface Science*. 2014;292:447-53. <https://doi.org/10.1016/j.apsusc.2013.11.158>
- Yuvaraja G, Chen D-Y, Pathak JL, Long J, Subbaiah MV, Wen J-C, et al. Preparation of novel aminated chitosan schiff's base derivative for the removal of methyl orange dye from aqueous environment and its biological applications. *International Journal of Biological Macromolecules*. 2020;146:1100-10. <https://doi.org/10.1016/j.ijbiomac.2019.09.236>
- Bal G, Thakur A. Distinct approaches of removal of dyes from wastewater: A review. *Materials Today: Proceedings*. 2022;50:1575-9. <https://doi.org/10.1016/j.matpr.2021.09.119>
- Sansuk S, Srijaranai S, Srijaranai S. A New Approach for Removing Anionic Organic Dyes from Wastewater Based on Electrostatically Driven Assembly. *Environmental Science & Technology*. 2016;50(12):6477-84. <https://doi.org/10.1021/acs.est.6b00919>
- Sharma S, Kaur A. Various methods for removal of dyes from industrial effluents-a review. *Indian J Sci Technol*. 2018;11(1). <https://doi.org/10.17485/ijst/2018/v11i12/120847>
- Azimi SC, Shirini F, Pendashteh AR. Advanced Oxidation Process as a Green Technology for Dyes Removal from Wastewater: A Review. *Iranian Journal of Chemistry and Chemical Engineering*. 2021;40(5):1467-89.
- Dassanayake R, Peramune D, Manatunga D, Premalal EVA, Nilmini R, Gunathilake C, et al. Recent advances in biopolymer-based advanced oxidation processes for dye removal applications: A review. *Environmental Research*. 2022;215:114242. <https://doi.org/10.1016/j.envres.2022.114242>
- Dutta S, Gupta B, Srivastava SK, Gupta AK. Recent advances on the removal of dyes from wastewater using various adsorbents: A critical review. *Materials Advances*. 2021;2(14):4497-531. <https://doi.org/10.1039/D1MA00354B>
- Lan D, Zhu H, Zhang J, Li S, Chen Q, Wang C, et al. Adsorptive removal of organic dyes via porous materials for wastewater treatment in recent decades: A review on species, mechanisms and perspectives. *Chemosphere*. 2022;293:133464. <https://doi.org/10.1016/j.chemosphere.2021.133464>
- Dieu Le T, Vinh Tran H. Graphene Oxide-Based Adsorbents for Organic-Dyes Removal from Contaminated Water: A Review. *Zeitschrift für anorganische und allgemeine Chemie*. 2022;648(18):e202200140. <https://doi.org/10.1002/zaac.202200140>
- Shi T-T, Jiang X-Y, Yu J-G. Efficient and Selective Removal of Organic Cationic Dyes by Peel of Brassica juncea Coss. var. gemmifera Lee et Lin-Based Biochar. *Molecules* [Internet]. 2023; 28(8). <https://doi.org/10.3390/molecules28083353>
- Elhami S, Abrishamkar M, Esmaeilzadeh L. Preparation and Characterization of Diethylenetriamine-montmorillonite and its application for the removal of Eosin Y dye: Optimization, Kinetic and Isotherm studies. *Journal of Scientific and Industrial Research*. 2013;72:461-6.
- Wu Y, Zhang S, Guo X, Huang H. Adsorption of chromium(III) on lignin. *Bioresource Technology*. 2008;99(16):7709-15. <https://doi.org/10.1016/j.biortech.2008.01.069>
- Bukhari A, Ijaz I, Zain H, Ezaz Gilani S, Nazir A, Bukhari A, et al. Removal of Eosin dye from simulated media onto lemon peel-based low cost biosorbent. *Arabian Journal of Chemistry*. 2022;15:103873. <https://doi.org/10.1016/j.arabjc.2022.103873>
- Salem M, Farid Y, Nosier S, Adli O, Abdel-Aziz MH. Removal of Eosin Yellow dye from industrial wastewater using UV/H<sub>2</sub>O<sub>2</sub> and photoelectro-Fenton techniques. *Journal of Photochemistry and Photobiology A: Chemistry*. 2022;436:114411. <https://doi.org/10.1016/j.jphotochem.2022.114411>
- Kooli F, Liu Y, Abboudi M, Rakass S, Oudghiri Hassani H, Ibrahim S, et al. Removal Properties of Anionic Dye Eosin by Cetyltrimethylammonium Organo-Clays: The Effect of Counter-Ions and Regeneration Studies. *Molecules*. 2018;23:2364. <https://doi.org/10.3390/molecules23092364>
- Kumar S, Balu K, Sobral A, Koh J. Bio-based (Chitosan/PVA/ZnO) nanocomposites film: Thermally stable and photoluminescence material for removal of organic dye. *Carbohydrate Polymers*. 2018;205. <https://doi.org/10.1016/j.carbpol.2018.10.108>
- Foroughnia A, Khalaji A, Kolvari E, Koukabi N. Synthesis of new chitosan Schiff base and its Fe<sub>2</sub>O<sub>3</sub> nanocomposite: Evaluation of methyl orange removal and antibacterial activity. *International Journal of Biological Macromolecules*. 2021;177. <https://doi.org/10.1016/j.ijbiomac.2021.02.068>
- Bashandeh Z, Khalaji AD. Effective removal of methyl green from aqueous solution using epichlorohydrine cross-linked chitosan. *Adv J Chem A*. 2021;4:270-7.
- Ai L, Zeng Y. Hierarchical porous NiO architectures as highly recyclable adsorbents for effective removal of organic dye from aqueous solution. *Chemical Engineering Journal*. 2013;215-216:269-78. <https://doi.org/10.1016/j.cej.2012.10.059>
- Wang J, Shao X, Zhang Q, Tian G, Ji X, Bao W. Preparation of mesoporous magnetic Fe<sub>2</sub>O<sub>3</sub> nanoparticle and its application for organic dyes removal. *Journal of Molecular Liquids*. 2017;248:13-8. <https://doi.org/10.1016/j.molliq.2017.10.026>
- Rahmi, Ishmaturrahmi, Mustafa I. Methylene blue removal from water using H<sub>2</sub>SO<sub>4</sub> crosslinked magnetic chitosan nanocomposite beads. *Microchemical Journal*. 2019;144:397-402.

- <https://doi.org/10.1016/j.microm.2018.09.032>
24. Zeraatkar Moghaddam A, Ghiamati E, Pourashuri A, Allahresani A. Modified nickel ferrite nanocomposite/functionalized chitosan as a novel adsorbent for the removal of acidic dyes. *International Journal of Biological Macromolecules*. 2018;120:1714-25. <https://doi.org/10.1016/j.ijbiomac.2018.09.198>
  25. Li W, Liu J, Qiu Y, Li C, Wang W, Yang Y. Polyethylene glycol modified magnetic nanoparticles for removal of heavy metal ions from aqueous solutions. *Journal of Dispersion Science and Technology*. 2019;40(9):1338-44. <https://doi.org/10.1080/01932691.2018.1511436>
  26. li C, She M, She X, Dai J, Kong L. Functionalization of Polyvinyl Alcohol Hydrogels with Graphene Oxide for Potential Dye Removal. *Journal of Applied Polymer Science*. 2014;131:39872. <https://doi.org/10.1002/app.39872>
  27. Huang C, Liao H, Ma X, Xiao M, Liu X, Gong S, et al. Adsorption performance of chitosan Schiff base towards anionic dyes: Electrostatic interaction effects. *Chemical Physics Letters*. 2021;780:138958. <https://doi.org/10.1016/j.cpl.2021.138958>
  28. Huo M-X, Jin Y-L, Sun Z-F, Ren F, Pei L, Ren P-G. Facile synthesis of chitosan-based acid-resistant composite films for efficient selective adsorption properties towards anionic dyes. *Carbohydrate Polymers*. 2021;254:117473. <https://doi.org/10.1016/j.carbpol.2020.117473>
  29. Yin M, Li X, Liu Y, Ren X. Functional chitosan/glycidyl methacrylate-based cryogels for efficient removal of cationic and anionic dyes and antibacterial applications. *Carbohydrate Polymers*. 2021;266:118129. <https://doi.org/10.1016/j.carbpol.2021.118129>
  30. Kale RD, Kane PB. Decolorization by PVP stabilized Fe-Ni nanoparticles of Reactive Black 5 dye. *Journal of Environmental Chemical Engineering*. 2018;6(5):5961-9. <https://doi.org/10.1016/j.jece.2018.09.015>
  31. Heddi D, Benkhaled A, Boussaid A, Choukhou-Braham E. Adsorption of Anionic Dyes on Poly(N-vinylpyrrolidone) Modified Bentonite. *Physical Chemistry Research*. 2019;7(4):731-49.
  32. Pandey G, Singh S, Hitkari G. Synthesis and characterization of polyvinyl pyrrolidone (PVP)-coated Fe<sub>3</sub>O<sub>4</sub> nanoparticles by chemical co-precipitation method and removal of Congo red dye by adsorption process. *International Nano Letters*. 2018;8(2):111-21. <https://doi.org/10.1007/s40089-018-0234-6>
  33. Suárez J, Daboin V, González G, Briceño S. Chitosan-polyvinylpyrrolidone CoxFe<sub>3</sub>-xO<sub>4</sub> (0.25 ≤ x ≤ 1) nanoparticles for hyperthermia applications. *International Journal of Biological Macromolecules*. 2020;164:3403-10. <https://doi.org/10.1016/j.ijbiomac.2020.08.043>
  34. Mondal D, Mollick MMR, Bhowmick B, Maity D, Bain MK, Rana D, et al. Effect of poly(vinyl pyrrolidone) on the morphology and physical properties of poly(vinyl alcohol)/sodium montmorillonite nanocomposite films. *Progress in Natural Science: Materials International*. 2013;23(6):579-87. <https://doi.org/10.1016/j.pnsc.2013.11.009>
  35. Topkaya R, Kurtan U, Baykal A, Toprak MS. Polyvinylpyrrolidone (PVP)/MnFe<sub>2</sub>O<sub>4</sub> nanocomposite: Sol-Gel autocombustion synthesis and its magnetic characterization. *Ceramics International*. 2013;39(5):5651-8. <https://doi.org/10.1016/j.ceramint.2012.12.081>
  36. Krishnan PG, Sobha A, Balakrishnan MP, Sumangala R. Synthesis and characterization of Ag/PVP nanocomposites by reduction method. *Open Access Library*. 2014;1:e519. <https://doi.org/10.4236/oalib.1100519>
  37. Agarwal T, Gupta K, Alam S, Zaidi M. Fabrication and characterization of iron oxide filled polyvinyl pyrrolidone nanocomposites. *Int J Compos Mater*. 2012;2:17-21. <https://doi.org/10.5923/j.cmaterials.20120203.01>
  38. Abdelghany AM, Mekhail MS, Abdelrazek EM, Aboud MM. Combined DFT/FTIR structural studies of monodispersed PVP/Gold and silver nano particles. *Journal of Alloys and Compounds*. 2015;646:326-32. <https://doi.org/10.1016/j.jallcom.2015.05.262>
  39. Chai J-H, Wu Q-S. Electrospinning preparation and electrical and biological properties of ferrocene/poly (vinylpyrrolidone) composite nanofibers. *Beilstein journal of nanotechnology*. 2013;4(1):189-97. <https://doi.org/10.3762/bjnano.4.19>
  40. Franco P, De Marco I. The Use of Poly (N-vinyl pyrrolidone) in the Delivery of Drugs: A Review. *Polymers*. 2020;12(5):1114. <https://doi.org/10.3390/polym12051114>
  41. Luo Y, Hong Y, Shen L, Wu F, Lin X. Multifunctional Role of Polyvinylpyrrolidone in Pharmaceutical Formulations. *AAPS PharmSciTech*. 2021;22(1):34. <https://doi.org/10.1208/s12249-020-01909-4>
  42. Kamari HM, Al-Hada NM, Saion E, Shaari AH, Talib ZA, Flaifel MH, et al. Calcined Solution-Based PVP Influence on ZnO Semiconductor Nanoparticle Properties. *Crystals* [Internet]. 2017; 7(2). <https://doi.org/10.3390/cryst7020002>
  43. Zhu K, Wang G, Zhang S, Du Y, Lu Y, Na R, et al. Preparation of organic-inorganic hybrid membranes with superior antifouling property by incorporating polymer-modified multiwall carbon nanotubes. *RSC Adv*. 2017;7:30564-72. <https://doi.org/10.1039/C7RA04248E>
  44. Khalaji AD, Mohammadi N, Emami M. NiO nanoparticles: Synthesis, characterization, and methyl green removal study. *Progress in Chemical Biochemical Research*. 2021;4(4):372-8.
  45. Sun W, Chen L, Meng S, Wang Y, Li H, Han Y, et al. Synthesis of NiO nanospheres with ultrasonic method for supercapacitors. *Materials Science in Semiconductor Processing*. 2014;17:129-33. <https://doi.org/10.1016/j.mssp.2013.09.002>
  46. Dehno Khalaji A. Preparation and Characterization of NiO Nanoparticles via Solid-State Thermal Decomposition of Ni(II) Complex. *Journal of Cluster Science*. 2013;24(1):189-95. <https://doi.org/10.1007/s10876-012-0542-3>
  47. Khalaji AD, Nikoogar M, Das D. Preparation and characterization of nickel oxide nanoparticles via solid state thermal decomposition of dinuclear nickel(II) Schiff base complex [Ni<sub>2</sub>(Brsal-1,3-ph)<sub>2</sub>] as a new precursor. *Research on Chemical Intermediates*. 2015;41(1):357-63. <https://doi.org/10.1007/s11164-013-1197-x>
  48. Huang X-Y, Bin J-P, Bu H-T, Jiang G-B, Zeng M-H. Removal of anionic dye eosin Y from aqueous solution using ethylenediamine modified chitosan. *Carbohydrate Polymers*. 2011;84(4):1350-6. <https://doi.org/10.1016/j.carbpol.2011.01.033>
  49. Yuvaraja G, Pang Y, Chen D-Y, Kong L-J, Mehmood S, Subbaiah MV, et al. Modification of chitosan macromolecule and its mechanism for the removal of Pb(II) ions from aqueous environment. *International*



- Journal of Biological Macromolecules. 2019;136:177-88.  
<https://doi.org/10.1016/j.ijbiomac.2019.06.016>
50. Zhang L, Hu P, Wang J, Huang R. Adsorption of Amido Black 10B from aqueous solutions onto Zr (IV) surface-immobilized cross-linked chitosan/bentonite composite. Applied Surface Science. 2016;369:558-66.  
<https://doi.org/10.1Wz016/j.apsusc.2016.01.217>